Inorganic Chemistry

Article

pubs.acs.org/IC

Probing the Role of Met221 in the Unusual Metallo-β-lactamase GOB-18

María-Natalia Lisa,[†,‡,§] Jorgelina Morán-Barrio,[†,‡] María-Fernanda Guindón,[†] and Alejandro J. Vila*[,†]

[†]Instituto de Biología Molecular y Celular de Rosario (IBR, CONICET-UNR) and Departamento de Química Biológica, Facultad de Ciencias Bioquímicas y Farmacéuticas, Universidad Nacional de Rosario, Ocampo y Esmeralda, Predio CONICET Rosario, 2000 Rosario, Argentina

Supporting Information

ABSTRACT: Metallo-β-lactamases (MβLs) are the main mechanism of bacterial resistance against last generation β-lactam antibiotics such as carbapenems. Most MβLs display unusual structural features in their active sites, such as binuclear zinc centers without carboxylate bridging ligands and/or a Cys ligand in a catalytic zinc site. Cys221 is an essential residue for catalysis conserved in B1 and B2 lactamases, while most B3 enzymes present a Ser in this position. GOB lactamases stand as an exception within this picture, with a Met residue in position 221. Then, we obtained a series of GOB-18 point mutants in order to analyze the role of this unusual Met221 residue. We found that Met221 is essential for the protein stability, most likely due to its involvement in a hydrophobic core. In contrast to other known MβLs, residue 221 is not involved in metal binding or in catalysis in GOB enzymes, according to spectroscopic and kinetic studies. Our findings show that the essential catalytic features are maintained despite the structural heterogeneity among MβLs and suggest that a strategy to design general inhibitors should be undertaken on the basis of mechanistic rather than structural information.

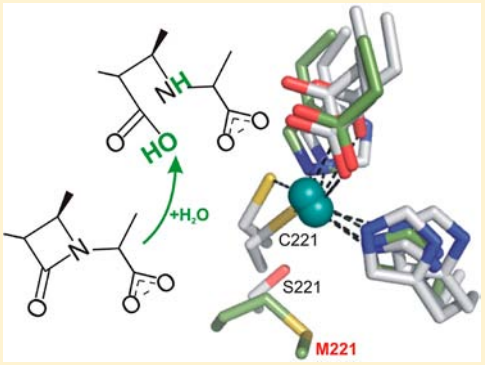

INTRODUCTION

The expression of β-lactam hydrolyzing enzymes (β-lactamases) is the most prevalent mechanism of bacterial resistance against β-lactam antibiotics.[1,2] Metallo-β-lactamases (MβLs) are zinc enzymes that catalyze the hydrolysis of most β-lactam antibiotics available on the drug market (including latest generation carbapenems) and which are resistant to all clinically employed inhibitors.[3−10] These facts together with the worldwide dissemination of MβL-encoding genes[11] constitute a distressing clinical problem. In addition, the design of an efficient pan-MβL inhibitor has been limited by the diversity in the active sites and the catalytic profiles among MβLs.[6,12−19]

MβLs have been classified into subclasses B1, B2, and B3, based on sequence identity.[10] All MβLs share a common αβ/βα fold able to host significantly different zinc coordination environments with variable metal occupancies (Figure 1).[12−19] MβLs are able to bind up to two metal ions in their active sites. In the broad spectrum B1 and B3 enzymes, Zn_1 is coordinated to three histidine ligands (His116, His118, and His196) and a water/OH^- molecule (the 3H site).[12−14,16,18−20] On the other hand, the coordination polyhedron of Zn_2 in B1 enzymes is provided by Asp120, Cys221, His263, and one or two water molecules (the DCH site).[13,14] Notably, a similar Zn_2 site forms the active species in mono-Zn(II) B2 enzymes (which hydrolyze only carbapenems).[15,17] Instead, two mutations (Cys221Ser and Arg121His) affect the Zn_2 coordination polyhedron in dinuclear B3MβLs, where the metal ion is bound to Asp120, His121, His263, and one or two water molecules (the DHH site), while Ser221 is no longer a metal ligand.[16,18,19] These metal centers are quite unusual when compared to canonical zinc hydrolases. First, dinuclear B1 and B3 lactamases lack a residue providing a bridging carboxylate, as found in most dinuclear hydrolases[21] and present instead a bridging hydroxide/water molecule. Second, B1 and B2 enzymes bear an essential Cys residue in a catalytic zinc site, which is rather uncommon, particularly given the fact that these enzymes are located in oxidizing environments such as the periplasmic space or the extracellular medium.

The recently described B3MβL GOB from *Elizabethkingia meningoseptica* represents an enigmatic case. The *gob* gene is actively expressed *in vivo* in the original host as a functional β-lactamase[23] and in *E. coli* cells confers β-lactam resistance when expressed as a recombinant gene.[24,25] In all reported GOB sequences, His116 and Ser221 are replaced by Gln and Met residues, respectively. While a His116Asn substitution in the exclusive carbapenemases B2 leads to a different metal binding site with inhibitory effects,[26] GOB has been shown to be active against a broad spectrum of β-lactam substrates either with one or two Zn(II) ions.[22,27,28] Surprisingly, the active mono-Zn(II) species presents the metal ion bound to the canonical Zn_2 (DHH) site of dinuclear B3MβLs (Figure 1).[22,27] Due to the lack of a 3D structure for a GOB variant, the impact of these unusual features in the activity of these enzymes still remains

Received: August 16, 2012
Published: October 31, 2012

 © 2012 American Chemical Society dx.doi.org/10.1021/ic301801h | *Inorg. Chem.* 2012, 51, 12419−12425

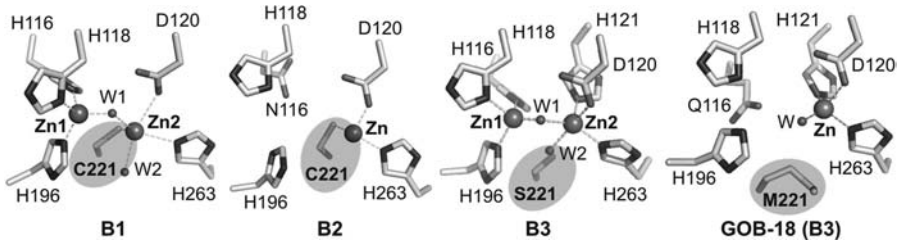

Figure 1. Metallo-β-lactamase metal binding sites. From left to right: dinuclear B1MβL BcII from *Bacillus cereus* (PDB 1bc2), mononuclear B2MβL CphA from *Aeromonas hydrophila* (PDB 1x8g), dinuclear B3MβL L1 from *Stenotrophomonas maltophilia* (PDB 1sml), and a molecular model for mononuclear B3MβL GOB-18 from *Elizabethkingia meningoseptica*.[22] Zinc atoms are shown as large gray spheres, and water molecules (W) are shown as small gray spheres. Coordination bonds are shown as dashed lines.

obscure and prompts for the use of mutagenesis and spectroscopy.

We have recently shown that only a hydrophobic and bulky residue can replace Met221 in GOB-18 and still provide a stable, processed enzyme in the periplasmic space, conferring antibiotic resistance to the bacterial host.[25] Extended X-ray absorption fine structure (EXAFS) studies on GOB-18 did not give any evidence of sulfur donor atoms in the coordination sphere of the metal ion, suggesting that Met221 is not a metal ligand in this enzyme.[22] However, Met binding to metals might be missed from EXAFS experiments given the usually long metal−S(Met) distances in metalloproteins. In an effort to assess the role of residue Met221 in GOB enzymes, we generated a series of GOB-18 mutants in this position. Here, we report the effect of the introduced substitutions on recombinant GOB-18 mutants, and a kinetic and spectroscopic characterization of mutant Met221Ile. We also show the activity of mutant Met221Ser. In the present work, we show evidence that Met221 is not essential for enzyme catalysis or metal binding. Instead, the hydrophobic and bulky nature of this residue is a key feature contributing to the enzyme stability.

EXPERIMENTAL SECTION

Culture Conditions. *E. coli* strains were grown aerobically, at 37 °C, in LB broth supplemented with kanamycin (50 μg/mL) and chloramphenicol (35 μg/mL) when necessary.

Chemicals. Biochemical reagents were purchased from Sigma-Aldrich except when another supplier is specified. Metal-free buffers were prepared adding Chelex 100 (Sigma) to normal buffers and stirring for half an hour.

Plasmid pET9a-GOB-18 and Derivatives. Plasmid pET9a-GOB-18 (which allows the overproduction of the fusion protein GST-GOB-18 in the cytoplasm of *E. coli* cells; GST: Glutathione S-transferase) was previously constructed[22] and contains a resistance marker for the antibiotic kanamycin. Plasmids pET9a-Met221X GOB-18 (X corresponds to Cys, Ser, His, Gln, Asp, Glu, or Ile) were generated by mutating the gene *gob-18* in vector pET9a-GOB-18.[25]

Expression of GOB-18 and Met221X GOB-18 Mutants. Protein expression was performed by employing the plasmid pET9a-GOB-18 and the derivatives pET9a-Met221X GOB-18, together with *E. coli* BL21 (DE3) Codon Plus RIL as the bacterial host. In each case, 5 mL cultures of transformed cells were grown until reaching 0.8−1 units of optical density at 600 nm. At this point, the expression of the corresponding fusion proteins was induced by the addition of lactose. Cells were harvested, and each pellet was resuspended in 900 μL of MTPBS buffer (16 mM Na_2HPO_4, 4 mM NaH_2PO_4, and 150 mM NaCl, pH 7.3) supplemented with DNase (0.1 μg/culture ml), $MgCl_2$ (5 mM), and phenylmethylsulfonyl fluoride (1 mM). Cells were then disrupted by sonication (13 cycles of 3 s of pulse and 30 s of waiting period, at 35 W) at 4 °C and subjected to ultracentrifugation at 100 000*g*, for 60 min, and at 4 °C. The resulting soluble fractions were stored at −20 °C. Insoluble fractions were stored under the same conditions, after resuspending each one in 900 μL of MTPBS buffer supplemented as described above. Induced whole cells and the corresponding soluble and insoluble cellular fractions were finally analyzed by SDS-PAGE and Coomassie Blue staining.

Enzyme Preparations. Met221Ile GOB-18 was produced by employing plasmid pET9a-Met221Ile GOB-18 and *E. coli* BL21 (DE3) Codon Plus RIL as the bacterial host. Protein induction was initiated by the addition of 0.25% w/v lactose to a bacterial culture of 0.8−1 units of optical density at 600 nm and later extended for 16−20 h at 15 °C. After harvesting the induced cells, Met221Ile GOB-18 purification was performed as previously described for the wild type enzyme.[22,27] Met221Ser GOB-18 was produced by employing plasmid pET9a-Met221Ser GOB-18, under identical conditions to the wild type enzyme. Mutant Met221Ser GOB-18 and wild type GOB-18 were purified as previously described.[22,27] In all cases, protein purity was higher than 95% (as determined by SDS-PAGE and Coomassie Blue staining), and the yields of pure recombinant proteins were of *ca.* 8, 8, and <0.17 mg per liter of bacterial culture for wild-type GOB-18, Met221Ile GOB-18, and Met221Ser GOB-18, respectively. Protein concentration was determined spectrophotometrically, employing $\varepsilon_{280\ nm}$ = 32 200 M^{-1} cm^{-1}.[22]

Metal Substitution. Apo-Met221Ile GOB-18 was obtained by employing EDTA as a chelating agent under mild denaturing conditions, as previously described for wild type GOB-18.[22,27] Metal removal was checked by atomic absorption spectroscopy. Zn(II)-Met221Ile GOB-18 and Co(II)-Met221Ile GOB-18 were prepared by dialyzing apo-Met221Ile GOB-18 against a metal containing buffer, as previously described for the wild type enzyme.[22,27] Zn(II)-GOB-18 was prepared as previously described.[22,27]

Metal Content Determination. Metal content determinations were performed with atomic absorption spectroscopy, using a Metrolab 250 instrument operating in the flame mode.

Electronic Absorption Spectroscopy. UV−vis spectra were recorded on a Jasco V-550 spectrophotometer, at 25 °C. Samples were in 15 mM HEPES at pH 7.5, 200 mM NaCl.

Nuclear Magnetic Resonance Spectroscopy (NMR). NMR spectra were recorded at 298 K on a Bruker Avance II 600 spectrometer operating at 600.13 MHz. ^{1}H NMR spectra were acquired under conditions to optimize the detection of the fast relaxing isotropically shifted resonances, either using the superWEFT pulse sequence[29] or water presaturation. These spectra were recorded over large spectral widths, with acquisition times ranging from 16 to 80 ms, and intermediate delays from 2 to 35 ms. Samples were in 15 mM HEPES at pH 7.5, 200 mM NaCl.

Circular Dichroism Spectroscopy. Samples were prepared by dialyzing the corresponding protein solutions twice against 300 volumes of 10 mM Tris-HCl at pH 7, 50 mM NaCl, for 8−12 h, at 4 °C. Measurements were performed using a Jasco J-715 spectropolarimeter flushed with N_2 and thermostatized with a Peltier element. Thermal unfolding experiments were performed by using a 4 °C/min ramp rate.

Nonsteady State Kinetics. Nitrocefin hydrolysis catalyzed by Zn(II)-Met221Ile GOB-18 was followed employing an SX.18-MVR stopped-flow spectrometer associated with a PD.1 photodiode array (Applied Photophysics, Surrey, U.K.) or an absorbance photo-

multiplier. All reactions were performed under single turnover conditions, in metal free 100 mM HEPES at pH 7.5, 200 mM NaCl, at 4 °C. Nonlinear regression analysis was used to fit single-wavelength absorbance changes with the program Dynafit.[30] Groups of data corresponding to the hydrolysis of different concentrations of nitrocefin were fitted simultaneously. The molar extinction coefficients of nitrocefin used were substrate $\varepsilon_{390\ nm}$ = 18 400 M^{-1} cm^{-1}; product $\varepsilon_{390\ nm}$ = 6300 M^{-1} cm^{-1}, $\varepsilon_{490\ nm}$ = 17 400 M^{-1} cm^{-1}, $\varepsilon_{665\ nm}$ = 500 M^{-1} cm^{-1}. Steady state kinetic parameters for the hydrolysis of nitrocefin catalyzed by Zn(II)-Met221Ile GOB-18 were calculated as $k_{cat} = k_2k_3/(k_2 + k_3)$ and $K_m = k_3\ (k_{-1} + k_2)/k_{+1}\ (k_2 + k_3)$.

Steady State Kinetics. All reactions were performed at 30 °C in 15 mM HEPES at pH 7.5, 200 mM NaCl. Antibiotic hydrolysis was monitored following the absorbance variation resulting from the hydrolysis of the β-lactam ring, using the following extinction coefficients: imipenem, $\Delta\varepsilon_{300\ nm}$ = −9000 M^{-1} cm^{-1}; penicillin G, $\Delta\varepsilon_{235\ nm}$ = −800 M^{-1} cm^{-1}; cefotaxime, $\Delta\varepsilon_{260\ nm}$ = −7500 M^{-1} cm^{-1}; and nitrocefin, $\Delta\varepsilon_{490\ nm}$ = 17 400 M^{-1} cm^{-1}. The kinetic parameters k_{cat} and K_m were derived from nonlinear fit of Michaelis−Menten equation to initial rate measurements recorded on a Jasco V-550 spectrophotometer, and the informed values correspond to the average obtained from at least two independent enzyme preparations. k_{cat} values have been calculated taking into account the concentration of metalated mononuclear enzyme.

RESULTS

Mutation of Residue Met221 in GOB-18 Is Destabilizing. In order to unravel the role of residue Met221 in GOB enzymes, we engineered different GOB-18 point mutants in this position. We decided to explore possible metal ligands, including the ubiquitous Cys present in B1 and B2 enzymes (Figure 1), the conserved Asp residue found in members of the MβL superfamily with no lactamase activity,[7,21] as well as His, Gln, and Glu. A Ser residue was also engineered to mimic the second shell ligand found in most B3 enzymes (Figure 1). We have already shown that these mutants are not able to confer antibiotic resistance to *E. coli*, suggesting that the activity and/or the stability of the enzyme are compromised by the substitutions.[25] On the contrary, mutant Met221Ile was the only variant able to confer appreciable levels of antibiotic resistance to the host,[25] so it was also included in the present study.

We decided to express and purify these mutants to assess the effect of the substitutions at the molecular level. We expressed the different GOB-18 variants in *E. coli* cells with plasmids pET9a-Met221X GOB-18, as already described for the wild type enzyme.[22,27] All variants expressed up to similar high levels, but only wild type GOB-18 was found in significant amounts in the soluble fraction, as revealed by SDS-PAGE and Coomassie Blue staining (Figure S1A). Instead, similar amounts of all Met221X GOB-18 mutants were found in inclusion bodies. Efforts were then made in order to find conditions allowing the production of Met221X GOB-18 mutants as soluble proteins. We attempted to reduce the rate of protein synthesis to minimize the formation of inclusion bodies by decreasing the amount of added inductor and the induction temperature. First, the inductor concentration was reduced to 0.25% w/v lactose, but only a slight increase in the solubility of the different Met221X GOB-18 variants was observed (Figure S1B). Then, the induction temperature was reduced to 15 °C, using 0.25−1% w/v lactose as the inductor. The soluble portion of the fusion proteins was not improved, except in the case of mutant Met221Ile GOB-18, for which a net increase in the amount of soluble protein was observed (Figure S1C). The levels of soluble Met221Ile GOB-18 obtained by inducing the protein expression at 15 °C with 0.25% w/v lactose were similar to those of wild type GOB-18 produced in the original conditions (Figure S1D).

The unsuccessful production of most Met221 mutants as soluble proteins and their accumulation as aggregates in inclusion bodies can be attributed to a destabilizing effect introduced by the mutations,[31] which is not operative in the case of Met221Ile (*i.e.*, substitution by a hydrophobic, isosteric residue). These results correlate very well with our previous *in vivo* experiments, which showed significantly diminished periplasmic levels for all mutants except for Met221Ile GOB-18.[25] This correlation suggests that the analyzed mutations destabilize the folded protein state, and we therefore decided to characterize in detail the stable Met221Ile mutant.

Spectroscopic Characterization of Met221Ile GOB-18 Mutant. Met221Ile GOB-18 was produced and purified to homogeneity as previously reported for the native enzyme,[22,27] with an average yield of 8 mg of pure recombinant protein per liter of bacterial culture. Atomic absorption analysis showed that purified holo-Met221Ile GOB-18 (the "as isolated" protein) contains 0.85 ± 0.02 Fe equivalents and 0.05 ± 0.02 Zn equivalents, resembling the situation described for holo-GOB-18.[22] The total metal content of the purified mutant never exceeded one metal equivalent/protein. It has been shown that, similarly, wild type GOB-18 binds iron better than zinc when overexpressed in the cytoplasm of *E. coli*, giving rise to a mixture of the mono-Fe(III) and mono-Zn(II) species with the metal ion located in the DHH site.[22] Despite the Zn(II) derivative being the native and active species, the Fe(III) derivative, although inactive, is more abundant in the enzyme purifications.[22] Holo-Met221Ile GOB-18 was poorly active, as expected by the dominant proportion of the inactive iron variant. The addition of extra Zn(II) to the reaction medium did not enhance the activity of holo-Met221Ile GOB-18, signaling that Zn(II) cannot displace the metal ion from the inactive Fe(III)-containing form. These observations indicate similar behavior to that previously found for wild type GOB-18.[22]

The spectroscopic features of the Fe(III)-bound protein have been shown to be a valuable tool to analyze the coordination sphere in the metal site of GOB-18.[22] The UV−visible spectrum of holo-Met221Ile GOB-18 revealed an absorption band centered at 375 nm, which was not present in the apoenzyme (metal-depleted) nor in the Zn(II)-reconstituted form (prepared as described in the Experimental Section; Figure 2A, data on wild type GOB-18 are shown in gray for facilitating comparison in each case). This feature is a typical His-Fe(III) charge transfer band, similar to that observed in wild type Fe(III)-GOB-18[22] and other nonheme, non-Fe-S iron proteins.[32] ^{1}H NMR spectra recorded under conditions that allow the detection of hyperfine shifted signals showed a set of resonances spanning from 110 to 20 ppm (Figure 2B). When the spectrum was recorded in D_2O, a loss of intensity corresponding to two protons was noticed in the broad envelope marked with an asterisk, indicating the presence of two exchangeable resonances, which can be attributed to two His ligands. These results closely resemble those previously reported for wild type GOB-18.[22]

We employed Co(II) as a surrogate of the zinc ion by adding Co(II) to the apoprotein (prepared as described in the Experimental Section).[20] The metal content of Co(II)-Met221Ile GOB-18 was of 0.6 ± 0.2 equivalents, according to atomic absorption measurements. The UV−visible spectrum

dx.doi.org/10.1021/ic301801h | *Inorg. Chem.* 2012, 51, 12419−12425

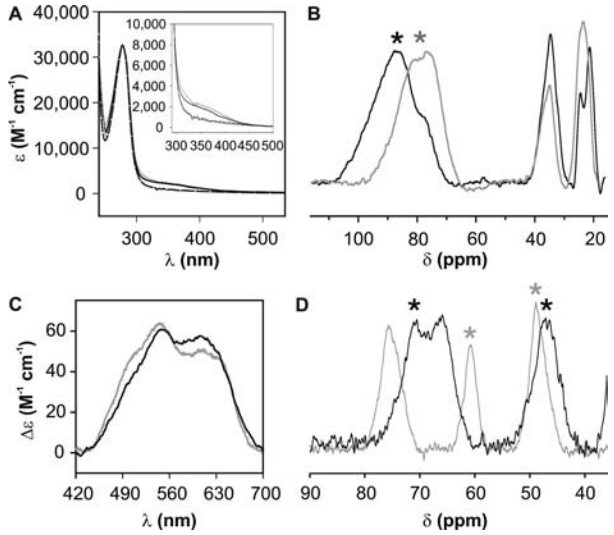

Figure 2. Fe(III) and Co(II)-Met221Ile GOB-18 spectroscopy characterization. In all cases, spectra corresponding to wild type GOB-18, acquired under the same experimental conditions (gray lines) are provided for comparison. (A) Electronic absorption spectrum of Fe(III) and apo-Met221Ile GOB-18 (black continuous line and black dashed line, respectively). Samples were in 15 mM HEPES at pH 7.5, 200 mM NaCl. Measurements were performed at 25 °C. (B) and (D) Fe(III)-Met221Ile GOB-18 and Co(II)-Met221Ile GOB-18 ^{1}H NMR spectra. Protein concentration was 1 mM. Samples were in 15 mM HEPES at pH 7.5, 200 mM NaCl, 10% D_2O. Measurements were performed at 298 K. The intensity of envelopes (*) diminished partially and totally in D_2O medium, respectively. Spectra were processed employing 300 and 200 Hz line broadenings, respectively. (C) Differential electronic absorption spectrum of Co(II)-Met221Ile GOB-18 minus apo-Met221Ile GOB-18. Samples were in 15 mM HEPES at pH 7.5, 200 mM NaCl. Measurements were performed at 25 °C.

of Co(II)-Met221Ile GOB-18 showed a set of transitions in the visible region, which are attributable to Laporte forbidden d−d (or ligand field) electronic transitions of the Co(II) ion bound to the protein[33] (Figure 2C). The molar extinction coefficient of these bands (50−60 M^{-1} cm^{-1}) is consistent with a pentacoordinated Co(II) ion.[33] A ^{1}H NMR spectrum of Co(II)-Met221Ile GOB-18 revealed a set of isotropically shifted resonances spanning from 80 to 40 ppm (Figure 2D). When similar spectra were run in D_2O, signals at 71 and 47 ppm were absent, indicating the presence of two solvent exchangeable resonances, which can be assigned to two His ligands. Thus, the spectroscopic features of Co(II)-Met221Ile GOB-18 are also similar to those corresponding to wild type Co(II)-GOB-18.[27] These results confirm that mutation Met221Ile introduces only minor structural perturbations in the metal binding site of the enzyme.

Thermal stability assays were performed on Zn(II)-Met221Ile GOB-18. This derivative was prepared as previously described,[22,27] and its metal content resulted in one zinc equivalent, identical to the situation met for the wild type enzyme.[22,27] The circular dichroism spectra of Zn(II)-Met221Ile GOB-18 in the far and near UV were nearly identical to those corresponding to wild type Zn(II)-GOB-18 (not shown), revealing similar secondary and tertiary structures in both cases. Thermal unfolding studies performed following the protein ellipticity at 222 nm upon heating revealed melting temperatures of 46.2 ± 0.6 °C for the mutant and 57.5 ± 0.7 °C for wild type Zn(II)-GOB-18 (not shown). This 11 °C decrease in T_m clearly evidences a destabilizing effect of Met221 substitution in GOB-18.

Kinetic Characterization of Met221Ile GOB-18 Mutant. The activity of Zn(II)-Met221Ile GOB-18 against a series of clinically relevant β-lactam antibiotics (a penicillin, a cephalosporin, and a carbapenem) was determined under steady state conditions. The kinetic parameters obtained are summarized in Table 1 and compared to those of wild type Zn(II)-GOB-18.[27] The addition of 20 μM Zn(II) to the reaction medium did not improve the catalytic efficiency of the mutant against the assayed substrates. Notably, mutation Met221Ile reduces the catalytic efficiency of GOB-18 against penicillin G by only a factor of 3, while it does not affect the hydrolysis of imipenem or cefotaxime. We also determined the steady state kinetic parameters of Co(II)-Met221Ile GOB-18 (summarized in Table 1 and compared to those of wild type Co(II)-GOB-18[27]). As can be noted, metal substitution mainly affects the values of the turnover constant, while the K_m remains within the same order of magnitude. This picture is identical to that previously observed for wild type GOB-18.[27]

We have recently reported the existence of an anionic intermediate in the hydrolysis of nitrocefin catalyzed by Zn(II)-GOB-18,[27] similar to that first reported by Benkovic and co-workers for the dinuclear enzyme CcrA from *Bacteroides fragilis*.[34,35] To evaluate the perturbations introduced in the

Table 1. Steady State Kinetic Parameters for the Hydrolysis of Different β-Lactam Substrates by Zn(II) and Co(II)−Met221Ile GOB-18

substrate			Penicillin G	Cefotaxime	Imipenem
Zn(II)	M221I	k_{cat} (s^{-1})	100 ± 20	35 ± 6	40 ± 7
		K_m (μM)	160 ± 20	44 ± 7	31 ± 5
		k_{cat}/K_m (s^{-1} μM^{-1})	0.6 ± 0.2	0.8 ± 0.3	1.3 ± 0.4
	WT[a]	k_{cat} (s^{-1})	700 ± 100	40 ± 10	34 ± 4
		K_m (μM)	360 ± 80	40 ± 9	28 ± 9
		k_{cat}/K_m (s^{-1} μM^{-1})	1.9 ± 0.4	1.1 ± 0.2	1.3 ± 0.4
Co(II)	M221I	k_{cat} (s^{-1})	9 ± 3	1.2 ± 0.2	2.7 ± 0.5
		K_m	110 ± 10	15 ± 3	30 ± 2
		k_{cat}/K_m (s^{-1} μM^{-1})	0.08 ± 0.03	0.08 ± 0.03	0.09 ± 0.02
	WT[a]	k_{cat} (s^{-1})	130 ± 10	5.8 ± 0.3	3.3 ± 0.2
		K_m (μM)	300 ± 100	33 ± 5	26 ± 6
		k_{cat}/K_m (s^{-1} μM^{-1})	0.4 ± 0.1	0.18 ± 0.03	0.13 ± 0.03

[a]The values corresponding to wild type GOB-18[27] are also given for comparison.

dx.doi.org/10.1021/ic301801h | *Inorg. Chem.* 2012, 51, 12419−12425

catalytic mechanism of GOB-18 by mutation Met221Ile, we followed the hydrolysis of nitrocefin mediated by Zn(II)-Met221Ile GOB-18 under pre-steady-state conditions. Figure 3A shows the progression of spectra obtained through the

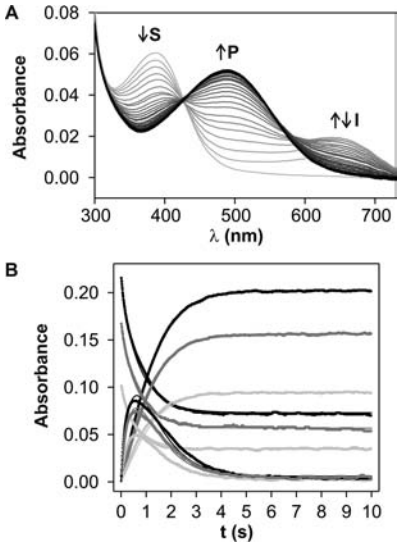

Figure 3. Non-steady-state nitrocefin hydrolysis catalyzed by Zn(II)-Met221Ile GOB-18. (A) Sequence of electronic absorption spectra of 3.3 μM nitrocefin upon reaction with 8.9 μM Zn(II)-Met221Ile GOB-18 obtained employing stopped flow equipment coupled to a photodiode array. Reaction progresses from gray to black spectra. (B) Time evolution of absorbance at 390, 490, and 665 nm upon reaction of (a) 11.6 μM nitrocefin with 18.9 μM Zn(II)-Met221Ile GOB-18 (black); (b) 9.0 μM nitrocefin with 18.9 μM Zn(II)-Met221Ile GOB-18 (dark gray); and (c) 5.5 μM nitrocefin with 18.9 μM Zn(II)-Met221Ile GOB-18 (light gray). In each case, 1000 points were recorded on a linear time scale over 10 s. Fits to the kinetic model in Scheme 1 overlay experimental points. Parameters obtained from the global fit of data: k_{+1} = 2.1 ± 0.2 s^{-1} μM^{-1}; k_{-1} = 380 ± 20 s^{-1}; k_2 = 13 ± 1 s^{-1}; k_3 = 2.318 ± 0.008 s^{-1}; ε_{EI} = 36 000 ± 2000 M^{-1} cm^{-1}. Measurements were performed in 100 mM HEPES at pH 7.5, 200 mM NaCl, at 4 °C. S, substrate; P, product; I, intermediate.

course of the reaction employing stopped flow equipment coupled to a photodiode array. Clearly, an intermediate species with a strong absorption band centered at 665 nm accumulates and then decays, analogous to what has been observed for Zn(II)-GOB-18.[27] Similar reactions with different substrate concentrations were then investigated following the evolution of the absorbance at 390, 490, and 665 nm, which are the absorption maxima of the substrate, product, and intermediate, respectively (Figure 3B).

The data obtained were simultaneously fitted to the mechanism depicted in Scheme 1:[27]

$$E + S \underset{k_{-1}}{\overset{k_{+1}}{\Leftrightarrow}} ES \overset{k_2}{\rightarrow} EI \overset{k_3}{\rightarrow} E + P \quad (1)$$

The individual kinetic constants resulting from this fit (summarized and compared to those of Zn(II)-GOB-18[27] in Table 2) were employed to calculate the steady state parameters, k_{cat} = 2.0 ± 0.3 s^{-1} and K_m = 28 ± 6 μM as described in the Experimental Section. These values compare very well with those determined under steady state conditions: k_{cat} = 1.34 ± 0.02 s^{-1} and K_m = 38 ± 2 μM, supporting the proposed model.

The kinetic results presented here show that mutation Met221Ile does not induce significant alterations neither in the catalytic efficiency nor in the catalytic mechanism of GOB-18.

In order to definitely discard a major influence of residue 221 on the enzyme activity, we decided to study mutant Met221Ser GOB-18. Substitution Met221Ser, which mimics the situation found in most B3MβLs (see Figure 1), severely impairs the production of a soluble, recombinant protein (Figure S1), and completely abrogates *gob-18*'s capability of conferring antibiotic resistance to *E. coli*.[25] We expressed and purified Met221Ser GOB-18, with very low yields (*ca.* 1 mg from a 6 L bacterial culture). The circular dichroism spectrum in the far UV (not shown) revealed a similar secondary structure upon the Met221Ser substitution. The zinc content of "as isolated" Met221Ser GOB-18 was of 0.15−0.20 metal equivalents, also similar to the situation found in the wild type enzyme.[22] The catalytic efficiency of Met221Ser GOB-18 against nitrocefin obtained by analysis of the complete time course of the reaction was 0.06 ± 0.02 μM^{-1} s^{-1}, revealing a less active variant by only a factor of 4 when compared to wild-type GOB-18. However, the low stability of this mutant precluded a more extended enzymatic characterization. These results show that substitution of Met221 by a smaller and hydrophilic Ser residue has only a very minor impact on GOB-18 activity. Actually, the effect of mutation Met221Ser on GOB-18 activity is in the same range as that observed for mutation Met221Ile (see Table 2). Then, these results allow us to reinforce the conclusion that residue Met221 is not essential for GOB-18 activity.

DISCUSSION

Position 221 is critical for the activity of all MβLs studied so far. In B1 and B2 enzymes, this residue is a conserved Cys which behaves as a metal ligand in the DCH site (Figure 1). A codon randomization study on the B1 lactamase IMP-1 identified Cys221 as an essential residue for activity,[36] and this has been confirmed for other B1 enzymes by site directed mutagenesis analysis.[37−39] Furthermore, we have recently shown that Cys221 is essential for the correct assembly of a dinuclear site in B1 enzymes in the periplasmic space.[39] Also, mutation of Cys221 to Ser or Ala in CphA results in a nearly inactive enzyme by abolishing the metal binding ability.[40] B3MβLs are evolutionarily more distant from B1 and B2 enzymes,[9] and they lack a Cys ligand in position 221. So far, all structurally characterized B3 lactamases possess a Ser residue in this position (Figure 1), which is involved in hydrogen bonding interactions with water molecules in the metal site. The Ser221Ala mutation in FEZ-1 was shown to selectively impair

Table 2. Kinetic Constants for the Hydrolysis of Nitrocefin by Zn(II)−Met221Ile GOB-18

	k_{+1} (s^{-1} μM^{-1})	k_{-1} (s^{-1})	k_2 (s^{-1})	k_3 (s^{-1})	k_{cat} (s^{-1})	K_m (μM)	k_{cat}/K_m (μM^{-1} s^{-1})
M221I	2.1 ± 0.2	380 ± 20	13 ± 1	2.318 ± 0.008	2.0 ± 0.3	28 ± 6	0.07 ± 0.02
WT[a]	4.8 ± 0.4	260 ± 20	14.1 ± 0.2	6.43 ± 0.02	4.4 ± 0.1	18 ± 3	0.24 ± 0.05

[a]The values corresponding to wild type GOB-18 [27] are also informed for comparison.

dx.doi.org/10.1021/ic301801h | *Inorg. Chem.* 2012, 51, 12419−12425

the carbapenemase activity.[16,41] Thus, in all hitherto studied MβLs, the residue in position 221 plays an important role in the enzyme activity, despite its identity and specific function.

GOB enzymes are unusual among MβLs, being the only enzymes possessing amino acid substitutions in consensus ligand positions within a subclass. Here, we have investigated the role of the native Met residue found in position 221 in all reported GOB natural variants. Several Met221X GOB-18 point mutants were generated, and the conditions for their production as recombinant proteins in *E. coli* were evaluated. Among all the amino acid residues analyzed, the replacement of methionine by isoleucine (an isosteric and hydrophobic residue) is the only one able to render a soluble and properly folded enzyme. Thus, substitution of Met221 by a hydrophilic residue impairs accumulation of soluble GOB-18 in the bacterial cytoplasm, and the effect seems to be most dramatic in the case of smaller residues (*i.e.*, Ser and Cys). These results, together with our previous *in vivo* studies,[25] strongly suggest that the hydrophobic and bulky nature of Met221 is a key feature contributing to the enzyme stability. To test this hypothesis, mutant Met221Ile GOB-18 and Met221Ser GOB-18 were purified for *in vitro* analysis.

Substitution Met221Ile did not affect the metal binding features of GOB-18. Moreover, as revealed by different spectroscopies, the metal binding site is largely unperturbed upon this mutation. Kinetic studies on this variant (both in the Zn(II) and the Co(II)-substituted forms) revealed that residue Met221 is not essential for the activity of GOB-18. This conclusion is also supported by data obtained for mutant Met221Ser GOB-18, which show that substitution of Met221 by a smaller and hydrophilic Ser residue has only a minor impact on GOB-18 activity, while eliciting a major effect on the stability of the mutant. Overall, these data suggest that Met221 residue might be located in a hydrophobic core within GOB-18 MβL.

These results are in agreement with previous EXAFS analysis, which did not provide evidence of a sulfur donor in the coordination sphere,[22] allowing us to definitively discard Met221 as a metal ligand. Also, the evidence presented here indicates that the catalytic site of GOB-18 remains mainly unperturbed upon Met221Ile substitution.

The stability of the Met221Ile GOB-18 mutant is clearly compromised, as revealed by protein unfolding data evidencing a decrease of 11 °C in the melting temperature as compared to the wild type enzyme. However, the enzyme is still within the stability threshold which ensures the production of a properly folded and soluble protein, in contrast to the situation observed for the other examined Met221 mutants. Thereby, replacement of Met221 by a bulky, hydrophobic amino acid is tolerated by the protein structure, suggesting that this residue is located within a hydrophobic cavity, with minimal or no interactions with the catalytic or the substrate binding site. Notably, this may also be the case for recently found B3MβLs containing residues Gln116/Met221 or Gln116/Ile221,[42,43] which originally led us to construct mutant Met221Ile GOB-18.[25]

The present analysis of the role of residue 221 in GOB enzymes reveals that this group of lactamases possesses a distinct active site topology, further highlighting the structural diversity among MβLs. However, the role of the consensus Zn_2 site (DHH site in GOB) in binding and orienting the substrate,[27,44] and stabilizing an anionic intermediate,[17,27,34,35,45−49] still stands as the common mechanistic feature in all MβLs and represents a target for inhibitor design.

■ ASSOCIATED CONTENT

Ⓢ Supporting Information

Expression of GST-Met221X GOB-18 recombinant mutants in *Escherichia coli* BL21 (DE3) Codon Plus RIL cells. This material is available free of charge via the Internet at http://pubs.acs.org.

■ AUTHOR INFORMATION

Corresponding Author

*Phone: +54-341-4237070 ext 632. Fax: +54-341-4390465. E-mail: vila@ibr-conicet.gov.ar.

Present Address

[§]Institut Pasteur, Unité de Microbiologie Structurale, CNRS URA 2185, 25 rue du Docteur Roux, 75724 Paris, France.

Author Contributions

[‡]These authors contributed equally to this work.

Notes

The authors declare no competing financial interest.

■ ACKNOWLEDGMENTS

M.-N.L. was recipient of a doctoral fellowship from CONICET. J.M.-B. is a staff member from CONICET and a former postdoctoral fellow of CONICET. A.J.V. is a staff member from CONICET. This work was supported by grants from ANPCyT and the U.S. National Institutes of Health (1R01AI100560) to A.J.V. The Bruker Avance II 600 MHz NMR spectrometer was purchased with funds from ANPCyT (PME2003-0026) and CONICET.

■ REFERENCES

(1) Fisher, J. F.; Meroueh, S. O.; Mobashery, S. *Chem. Rev.* **2005**, *105*, 395−424.

(2) Perez, F.; Endimiani, A.; Hujer, K. M.; Bonomo, R. A. *Curr. Opin. Pharmacol.* **2007**, *7*, 459−469.

(3) Cricco, J. A.; Rasia, R. M.; Orellano, E. G.; Ceccarelli, E. A.; Vila, A. J. *Coord. Chem. Rev.* **1999**, *190−192*, 519−535.

(4) Cricco, J. A.; Vila, A. J. *Curr. Pharm. Des* **1999**, *5*, 915−927.

(5) Walsh, T. R.; Toleman, M. A.; Poirel, L.; Nordmann, P. *Clin. Microbiol. Rev.* **2005**, *18*, 306−325.

(6) Crowder, M. W.; Spencer, J.; Vila, A. J. *Acc. Chem. Res.* **2006**, *39*, 721−728.

(7) Bebrone, C. *Biochem. Pharmacol.* **2007**, *74*, 1686−1701.

(8) Galleni, M.; Lamotte-Brasseur, J.; Rossolini, G. M.; Spencer, J.; Dideberg, O.; Frere, J. M. *Antimicrob. Agents Chemother.* **2001**, *45*, 660−663.

(9) Hall, B. G.; Salipante, S. J.; Barlow, M. *J. Mol. Evol.* **2003**, *57*, 249−254.

(10) Frere, J. M.; Galleni, M.; Bush, K.; Dideberg, O. *J. Antimicrob. Chemother.* **2005**, *55*, 1051−1053.

(11) Kumarasamy, K. K.; Toleman, M. A.; Walsh, T. R.; Bagaria, J.; Butt, F.; Balakrishnan, R.; Chaudhary, U.; Doumith, M.; Giske, C. G.; Irfan, S.; Krishnan, P.; Kumar, A. V.; Maharjan, S.; Mushtaq, S.; Noorie, T.; Paterson, D. L.; Pearson, A.; Perry, C.; Pike, R.; Rao, B.; Ray, U.; Sarma, J. B.; Sharma, M.; Sheridan, E.; Thirunarayan, M. A.; Turton, J.; Upadhyay, S.; Warner, M.; Welfare, W.; Livermore, D. M.; Woodford, N. *Lancet Infect. Dis.* **2010**, *10*, 597−602.

(12) Carfi, A.; Pares, S.; Duee, E.; Galleni, M.; Duez, C.; Frere, J. M.; Dideberg, O. *EMBO J.* **1995**, *14*, 4914−4921.

(13) Fabiane, S. M.; Sohi, M. K.; Wan, T.; Payne, D. J.; Bateson, J. H.; Mitchell, T.; Sutton, B. J. *Biochemistry* **1998**, *37*, 12404−12411.

(14) Concha, N. O.; Rasmussen, B. A.; Bush, K.; Herzberg, O. *Structure* **1996**, *4*, 823−836.

(15) Garau, G.; Bebrone, C.; Anne, C.; Galleni, M.; Frere, J. M.; Dideberg, O. *J. Mol. Biol.* **2005**, *345*, 785−795.

(16) Garcia-Saez, I.; Mercuri, P. S.; Papamicael, C.; Kahn, R.; Frere, J. M.; Galleni, M.; Rossolini, G. M.; Dideberg, O. *J. Mol. Biol.* **2003**, *325*, 651−660.
(17) Fonseca, F.; Bromley, E. H.; Saavedra, M. J.; Correia, A.; Spencer, J. *J. Mol. Biol.* **2011**, *411*, 951−959.
(18) Ullah, J. H.; Walsh, T. R.; Taylor, I. A.; Emery, D. C.; Verma, C. S.; Gamblin, S. J.; Spencer, J. *J. Mol. Biol.* **1998**, *284*, 125−136.
(19) Docquier, J. D.; Benvenuti, M.; Calderone, V.; Stoczko, M.; Menciassi, N.; Rossolini, G. M.; Mangani, S. *Antimicrob. Agents Chemother.* **2010**, *54*, 4343−4351.
(20) Orellano, E. G.; Girardini, J. E.; Cricco, J. A.; Ceccarelli, E. A.; Vila, A. J. *Biochemistry* **1998**, *37*, 10173−10180.
(21) Daiyasu, H.; Osaka, K.; Ishino, Y.; Toh, H. *FEBS Lett.* **2001**, *503*, 1−6.
(22) Moran-Barrio, J.; Gonzalez, J. M.; Lisa, M. N.; Costello, A. L.; Peraro, M. D.; Carloni, P.; Bennett, B.; Tierney, D. L.; Limansky, A. S.; Viale, A. M.; Vila, A. J. *J. Biol. Chem.* **2007**, *282*, 18286−18293.
(23) Gonzalez, L. J.; Vila, A. J. *Antimicrob. Agents Chemother.* **2012**, *56*, 1686−1692.
(24) Moran-Barrio, J.; Limansky, A. S.; Viale, A. M. *Antimicrob. Agents Chemother.* **2009**, *53*, 2908−2917.
(25) Moran-Barrio, J.; Lisa, M. N.; Vila, A. J. *Antimicrob. Agents Chemother.* **2012**, *56*, 1769−1773.
(26) Costello, A. L.; Sharma, N. P.; Yang, K. W.; Crowder, M. W.; Tierney, D. L. *Biochemistry* **2006**, *45*, 13650−13658.
(27) Lisa, M. N.; Hemmingsen, L.; Vila, A. J. *J. Biol. Chem.* **2010**, *285*, 4570−4577.
(28) Horsfall, L. E.; Izougarhane, Y.; Lassaux, P.; Selevsek, N.; Lienard, B. M.; Poirel, L.; Kupper, M. B.; Hoffmann, K. M.; Frere, J. M.; Galleni, M.; Bebrone, C. *FEBS J.* **2011**, *278*, 1252−1263.
(29) Inubushi, T.; Becker, E. D. *J. Magn. Reson.* **1983**, *51*, 128−133.
(30) Kuzmic, P. *Anal. Biochem.* **1996**, *237*, 260−273.
(31) Tyedmers, J.; Mogk, A.; Bukau, B. *Nat. Rev. Mol. Cell Biol.* **2010**, *11*, 777−788.
(32) Averill, B. A.; Vincent, J. B. *Methods Enzymol.* **1993**, *226*, 33−51.
(33) Maret, W.; Vallee, B. L. *Methods Enzymol.* **1993**, *226*, 52−71.
(34) Wang, Z.; Fast, W.; Benkovic, S. J. *J. Am. Chem. Soc.* **1998**, *120*, 10788−10789.
(35) Wang, Z.; Fast, W.; Benkovic, S. J. *Biochemistry* **1999**, *38*, 10013−10023.
(36) Materon, I. C.; Palzkill, T. *Protein Sci.* **2001**, *10*, 2556−2565.
(37) Paul-Soto, R.; Bauer, R.; Frere, J. M.; Galleni, M.; Meyer-Klaucke, W.; Nolting, H.; Rossolini, G. M.; de, S. D.; Hernandez-Valladares, M.; Zeppezauer, M.; Adolph, H. W. *J. Biol. Chem.* **1999**, *274*, 13242−13249.
(38) Haruta, S.; Yamaguchi, H.; Yamamoto, E. T.; Eriguchi, Y.; Nukaga, M.; O'Hara, K.; Sawai, T. *Antimicrob. Agents Chemother.* **2000**, *44*, 2304−2309.
(39) Gonzalez, J. M.; Meini, M. R.; Tomatis, P. E.; Martin, F. J.; Cricco, J. A.; Vila, A. J. *Nat. Chem. Biol.* **2012**, *8*, 698−700.
(40) Vanhove, M.; Zakhem, M.; Devreese, B.; Franceschini, N.; Anne, C.; Bebrone, C.; Amicosante, G.; Rossolini, G. M.; Van, B. J.; Frere, J. M.; Galleni, M. *Cell. Mol. Life Sci.* **2003**, *60*, 2501−2509.
(41) Mercuri, P. S.; Garcia-Saez, I.; De, V. K.; Thamm, I.; Devreese, B.; Van, B. J.; Dideberg, O.; Rossolini, G. M.; Frere, J. M.; Galleni, M. *J. Biol. Chem.* **2004**, *279*, 33630−33638.
(42) Ward, N. L.; Challacombe, J. F.; Janssen, P. H.; Henrissat, B.; Coutinho, P. M.; Wu, M.; Xie, G.; Haft, D. H.; Sait, M.; Badger, J.; Barabote, R. D.; Bradley, B.; Brettin, T. S.; Brinkac, L. M.; Bruce, D.; Creasy, T.; Daugherty, S. C.; Davidsen, T. M.; DeBoy, R. T.; Detter, J. C.; Dodson, R. J.; Durkin, A. S.; Ganapathy, A.; Gwinn-Giglio, M.; Han, C. S.; Khouri, H.; Kiss, H.; Kothari, S. P.; Madupu, R.; Nelson, K. E.; Nelson, W. C.; Paulsen, I.; Penn, K.; Ren, Q.; Rosovitz, M. J.; Selengut, J. D.; Shrivastava, S.; Sullivan, S. A.; Tapia, R.; Thompson, L. S.; Watkins, K. L.; Yang, Q.; Yu, C.; Zafar, N.; Zhou, L.; Kuske, C. R. *Appl. Environ. Microbiol.* **2009**, *75*, 2046−2056.
(43) Allen, H. K.; Moe, L. A.; Rodbumrer, J.; Gaarder, A.; Handelsman, J. *ISME.J.* **2009**, *3*, 243−251.
(44) Rasia, R. M.; Vila, A. J. *J. Biol. Chem.* **2004**, *279*, 26046−26051.
(45) Gonzalez, J. M.; Medrano Martin, F. J.; Costello, A. L.; Tierney, D. L.; Vila, A. J. *J. Mol. Biol.* **2007**, *373*, 1141−1156.
(46) Spencer, J.; Read, J.; Sessions, R. B.; Howell, S.; Blackburn, G. M.; Gamblin, S. J. *J. Am. Chem. Soc.* **2005**, *127*, 14439−14444.
(47) Tioni, M. F.; Llarrull, L. I.; Poeylaut-Palena, A. A.; Marti, M. A.; Saggu, M.; Periyannan, G. R.; Mata, E. G.; Bennett, B.; Murgida, D. H.; Vila, A. J. *J. Am. Chem. Soc.* **2008**, *130*, 15852−15863.
(48) Tomatis, P. E.; Fabiane, S. M.; Simona, F.; Carloni, P.; Sutton, B. J.; Vila, A. J. *Proc. Natl. Acad. Sci. U. S. A.* **2008**, *105*, 20605−20610.
(49) Zhang, H.; Hao, Q. *FASEB J.* **2011**, *25*, 2574−2582.